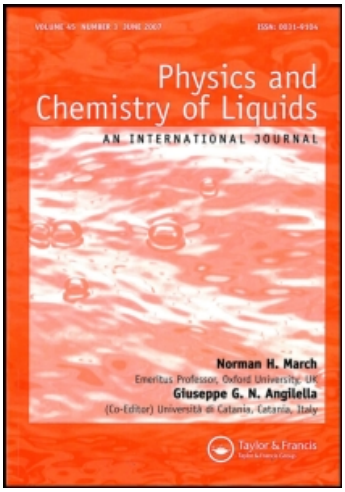

Physics and Chemistry of Liquids
Publication details, including instructions for authors and subscription information:
http://www.informaworld.com/smpp/title~content=t713646857

Structure of molten bismuth-copper alloys by means of thermal neutron diffraction in the momentum range of $k < 1$ å$^{-1}$

Werner Zaiss[ab]; Siegfried Steeb[a]
[a] Max-Planck-Institut für Metallforschung, Institut für Werkstoffwissenschaften, Stuttgart, Western Germany [b] University of Stuttgart,

Online publication date: 18 October 2010

To cite this Article Zaiss, Werner and Steeb, Siegfried(1976) 'Structure of molten bismuth-copper alloys by means of thermal neutron diffraction in the momentum range of $k < 1$ å$^{-1}$', Physics and Chemistry of Liquids, 6: 1, 1 — 19
To link to this Article: DOI: 10.1080/00319107608085057
URL: http://dx.doi.org/10.1080/00319107608085057

Phys. Chem. Liq., 1976, Vol. 6, pp. 1–19

Printed in Dordrecht, Holland

Structure of Molten Bismuth-Copper Alloys by Means of Thermal Neutron Diffraction in the Momentum Range of $\kappa > 1\ \text{Å}^{-1}$

WERNER ZAISS†

and

SIEGFRIED STEEB

Max-Planck-Institut für Metallforschung, Institut für Werkstoffwissenschaften, Stuttgart, Western Germany

(Received April 12, 1976)

Conventional diffraction experiments using thermal neutrons were performed in the range of momentum transfer between 1 Å^{-1} and 8 Å^{-1} over the total concentration range of the Bi-Cu system. The coherent differential scattering cross section of each liquid alloy was determined and compared with models. The structure of the molten pure elements copper and bismuth as well as of those alloys containing only 10 or 20 at. % of the second component can be described by hard-sphere models.

The alloys in the concentration range between 30 and 70 at. % Cu differ clearly from this model; their experimental scattering cross sections in the range of the first intensity maximum always vary between the extreme models of macroscopic segregation and random distribution of the atoms.

Using the Fourier transform of the total structure factors of the alloys as well as of the pure components, the nearest neighbour distance and the coordination number were determined. The concentration dependence of the nearest-neighbour distance doesn't give clear evidence with regard to the atomic arrangement. The number of atoms in the first coordination sphere, however, differs distinctly from that of the random distribution. From this difference it can be deduced that molten Bi-Cu-alloys show a tendency to segregation.

† Part of the thesis work of W. Zaiss, University of Stuttgart, 1975.

1 INTRODUCTION

In recent years structural analysis of binary liquid alloys was extended mainly to systems showing some particular structural properties[1].

The first group covers the compound-forming systems with intermetallic compounds in the solid state. These exhibit some short-range order in the liquid state, as can be concluded from the so-called premaxima in the intensity curves, observed for the first time with the Mg-Sn system[2] and often reported since then (Li-Pb[3], for example).

The second group covers systems with a tendency to segregation. The homogeneous phase of these liquids shows a certain degree of segregation within atomic dimensions: in the melts of these binary alloys so-called clusters exist which contain mainly atoms of the same species. These clusters give rise to scattering in the range of small momentum transfer such that the intensity increases towards the position of the primary beam. As examples the Al-Sn[4], Al-In[5], and Na-Li[6] systems should be mentioned.

According to Sauerwald[7], molten alloys of the Bi-Cu system should show a tendency to segregation. From the behaviour of the structure factor, the magnetic susceptibility, and the electrical resistivity in connection with model calculations, Takeuchi *et al.*[8] came to the conclusion that the atoms of different kinds are distributed randomly in these liquid alloys.

From measurements of the velocity of sound and density of the Bi-Cu system the partial structure factors could be determined for the long-wavelength limit in Ref.[9]. As a consequence of these studies it could be shown that inhomogeneities must exist in these melts.

During the present work the structure of molten Bi-Cu alloys was investigated over the entire concentration range by means of conventional neutron diffraction. Another investigation[10] in which scattering experiments with cold neutrons were performed in the momentum range $\kappa < 1{,}5\ \text{Å}^{-1}$ to get information about the size and the concentration of the inhomogenities supposed in Ref.[9] should be mentioned.

2 THEORETICAL FRAMEWORK

Scattering of neutrons from an ensemble of N atoms, where the energy loss or gain of the radiation due to thermal excitations must be considered, is described in the first Born approximation by the double differential scattering cross section per atom[11]:

$$\frac{d^2\sigma}{d\Omega d\omega} = \frac{1}{N}\frac{k_1}{k_0}\sum_{n,n'=1}^{N} a_n a_{n'} \cdot \frac{1}{2\pi}\int_{-\infty}^{+\infty} dt\, e^{-i\omega t}\langle e^{i\kappa[r_n(0)-r_{n'}(t)]}\rangle \qquad (1)$$

with $\hbar\underline{\kappa}$ = momentum transfer to the scattering system
k_1 = magnitude of the wave vector of the scattered neutrons
k_0 = magnitude of the wave vector of incoming neutrons

Also, a_n is the scattering length of the nucleus n at the position $\underline{r}_n$; $\underline{r}_n(t)$ is a time-dependent position vector and $\langle \ldots . \rangle$ means thermal average for the scattering system. The interaction between the scattering system and scattered radiation, e.g. between nucleus and neutron, is described only by the scattering-lengths, yet the cross section is determined by correlations in space and time between the scattering centres.

In the case of the quasielastic approximation[11], integration of Eq. (1) yields:

$$\frac{d\sigma(\kappa)}{d\Omega} = \int_{\substack{-\infty \\ \kappa=\text{const.}}}^{+\infty} \frac{d^2\sigma}{d\Omega d\omega} d\omega = \frac{1}{N} \sum_{n,n'=1} a_n a_{n'} \cdot \langle e^{i\underline{\kappa}(\underline{r}_n - \underline{r}_{n'})} \rangle \tag{2}$$

In the quasielastic approximation, the energy E_0 of the incoming neutrons is much larger than the energy transfer $\hbar\omega$ to the scattering system. Therefore, $k_1 \approx k_0$ and $\kappa = \frac{4\pi \sin\theta}{\lambda_0}$. The scattering angle between incoming and scattered radiation is 2θ, λ_0 being the wavelength of incoming neutrons.

The scattering lengths a_n and $a_{n'}$, depend on the relative orientation of nuclear and neutron spin and are different for the individual isotopes of one element. Since generally the isotopes as well as the different spin orientations are distributed randomly in the sample, the cross section is separated into a coherent and an incoherent part:

$$\frac{d\sigma(\kappa)}{d\Omega} = \left.\frac{d\sigma(\kappa)}{d\Omega}\right|_{COH} + \left.\frac{d\sigma}{d\Omega}\right|_{INC} \tag{3}$$

The incoherent part is calculated in Eq. (4):

$$\left.\frac{d\sigma}{d\Omega}\right|_{INC} = \frac{1}{4\pi}\left[c_1\sigma_{INC,1} + c_2\sigma_{INC,2}\right] \tag{4}$$

with $c_{1,2}$ = atomic concentration of element 1,2
$\sigma_{INC_{1,2}}$ = incoherent scattering cross section of element 1,2

In the case of a binary liquid, e.g. of an isotropic scattering system, the differential coherent scattering cross section is calculated as follows:

$$\left.\frac{d\sigma(\kappa)}{d\Omega}\right|_{COH} = c_1c_2(b_1 - b_2)^2 + \langle b\rangle^2\left(1 + \rho_0\int_0^\infty [g(r) - 1]\cdot 4\pi r^2 \frac{\sin \kappa r}{\kappa r} dr\right) \tag{5}$$

with $b_{1,2}$ = coherent scattering length of element 1,2

$\langle b \rangle = c_1 b_1 + c_2 b_2$

$\rho_0 = \frac{D_M \cdot N_L}{\overline{A}}$ = average atomic density

D_M = macroscopic density of the molten alloy

N_L = Avogadro's number

$\overline{A}$ = average atomic weight of the alloy

$g(r)$ = total pair correlation function

The first term in Eq. (5) represents the so-called Laue monotonic scattering and is nonzero for alloys containing more than one element with different coherent scattering lengths. The total structure factor $I(\kappa)$ is obtained from Eq. (5):

$$I(\kappa) = \frac{\left.\frac{d\sigma(\kappa)}{d\Omega}\right|_{COH} - c_1 c_2 (b_1 - b_2)^2}{\langle b \rangle^2} \tag{6}$$

Following Faber and Ziman[13], $I(\kappa)$ is defined by

$$I(\kappa) = \frac{c_1^2 b_1^2}{\langle b \rangle^2} a_{11}(\kappa) + \frac{c_2^2 b_2^2}{\langle b \rangle^2} a_{22}(\kappa) + \frac{2 c_1 c_2 b_1 b_2}{\langle b \rangle^2} a_{12}(\kappa) \tag{7}$$

The partial structure factors $a_{ij}(\kappa)$ describe respectively the scattering contribution of the i-j pairs to the total structure factor.

Using the Fourier transform the total pair correlation function $g(r) = \rho(r)/\rho_0$ and therefore the radial density function $\rho(r)$ is obtained from Eq. (6). The curve of $g(r)$ versus r yields the radius r_1 of the first coordination sphere, whereas from the shape of the atomic distribution function $4\pi r^2 \rho(r)$ the coordination number N_1 of the first sphere can be calculated. It should be stressed that the coordination number N_1, the distance r_1, the total structure factor $I(\kappa)$ as well as the total pair correlation function $g(r)$ are still dependent on the radiation used during the scattering experiment.

3 EXPERIMENTAL OUTLINE

The diffraction experiments were performed with thermal neutrons ($\lambda_0 = 1.2$ Å) at the Research Reactor FR2 of the Kernforschungszentrum Karlsruhe using a neutron diffractometer which is described in detail in Ref.[14].

The cylindrical specimen was centered in a high-temperature scattering furnace providing a temperature at the sample of up to 1300° C with a variation of ±1° C in a vacuum of 10^{-5} torr. The current in the vacuum heating tube was about 400 amp using a high-current transformer. Neutrons were

detected in four BF_3 counters installed on a detector carriage with a fixed distance of $2\theta = 15°$. The apparatus works automatically by tape control in steps of 0.2° in the region $5° < 2\theta < 120°$. The neutron flux amounts to 6.10^6 n/sec·cm² at the sample. The measuring time per sample was about 16–18 hours at a constant monitor preselection of 10^6 pulses, the statistical error being less than 2%.

The samples were investigated at temperatures 20° C above the liquidus, and to correct for absorption their transmission had to be determined. To calculate the background scattering, the intensity of the empty cell and the cell filled with Cd had to be measured. The geometry of installation was unchanged for all measurements.

Eleven specimens were prepared for the diffraction experiments, namely the pure elements Bi and Cu as well as nine alloys with concentrations at equal intervals over the total concentration range of the Bi-Cu system. As initial substances, copper (99.9%, granulated) and arsenic-free Bi were used. The specimens were melted in a vacuum induction furnace and cast in a graphite mold with a diameter of 8 mm and height of 70 mm. Then the specimens were refined in methanol by ultrasonics and sealed in evacuated silicon tubes. After performation of the diffraction experiments, the specimens were analyzed by means of X-ray fluoresence. The deviation from the weighted original sample was always less than 1%. To evaluate the measurements, scattering lengths and scattering cross sections of Bi and Cu were needed (see Table 1).

The background scattering I_B consists of two parts: the background scattering of the surroundings, and the background scattering of the furnace and the cell. The intensity $I_K(\kappa)$, corrected for background scattering and for absorption in the specimen, can be described as follows:

$$I_K(\kappa) = [I_{Exp}(\kappa) - I_B(\kappa)]/A \tag{8}$$

$I_{Exp}(\kappa)$ stands for the measured intensity of the molten sample; $I_B(\kappa)$ is the total background scattering[18]. "A" is the absorption coefficient, which is

TABLE I

Scattering lengths and scattering cross sections for Bi and Cu

	dimension	Bi	Cu	reference
b	10^{-12} cm	0.852	0.76	15
σ_{INC}	10^{-24} cm²	—	0.58	16
σ_{ABS} ($\lambda_0 = 1.08$ Å)	10^{-24} cm²	0.02	2.2	17

defined in Ref.[19] and depends on 2θ and the product $R \cdot \Sigma$. R is the radius of the sample and Σ is called the attenuation coefficient, which was determined directly from transmission experiments. A correction for multiple scattering was performed following Blech and Averbach[20], the scattering cross section for multiple scattering being defined as follows:

$$\left.\frac{d\sigma}{d\Omega}\right|_{MSC} = \frac{1}{4\pi} \cdot \frac{\sigma_{SC}\left(\frac{\sigma_{SC}}{\sigma_t}\right)\delta}{1 - \left(\frac{\sigma_{SC}}{\sigma_t}\right)\delta} \tag{9}$$

The coefficient δ is tabulated in Ref.[20] for different R/h ratios as a function of $R \cdot \Sigma$. "h" is defined as the height of the incoming neutron beam at the sample, σ_{SC} is calculated according to Eq. (10):

$$\sigma_{SC} = \frac{\Sigma}{\rho_0} - \sigma_{ABS} = \sigma_t - \sigma_{ABS} \tag{10}$$

with σ_{ABS} = cross section of absorption (see Table 1).

A correction for inelastic effects (Placzek[21]) could be neglected for the present combination of Bi and Cu. The calculated intensity I_K is related to the differential coherent scattering cross section by Eq. (11):

$$\left.\frac{d\sigma(\kappa)}{d\Omega}\right|_{COH} = \beta_N \cdot I_K^{(\kappa)} - \left(\left.\frac{d\sigma}{d\Omega}\right|_{INC} + \left.\frac{d\sigma}{d\Omega}\right|_{MSC}\right) \tag{11}$$

The normalization coefficient β_N is defined in Eq. (12), using the method of Krogh-Moe[22]:

$$\beta_N = \frac{\frac{\kappa_{MAX}^3}{3} \cdot \left\{\left.\frac{d\sigma}{d\Omega}\right|_{INC} + \left.\frac{d\sigma}{d\Omega}\right|_{MSC} + \langle b^2\rangle\right\} - 2\pi^2\rho_0\langle b\rangle^2}{\int_0^{\kappa MAX} \kappa^2 \cdot I_K(\kappa)d\kappa} \tag{12}$$

with $\langle b^2\rangle = c_1 b_1^2 + c_2 b_2^2$.

Since the diffraction experiments can only be performed up to κ_{MAX}, this value is used as the upper integration limit.

4 RESULTS AND DISCUSSION

1 The pure elements Bi and Cu

Figs. 1a and 1b show the intensity pattern of the elements Bi and Cu on an absolute scale in the momentum range $1\ \text{Å}^{-1} < \kappa < 8\ \text{Å}^{-1}$. The values of b^2, to which the curves are normalized, are also plotted. The intensity curve of pure Bi at 800° C has its first maximum at $\kappa_M = 2.2\ \text{Å}^{-1}$, in agreement with

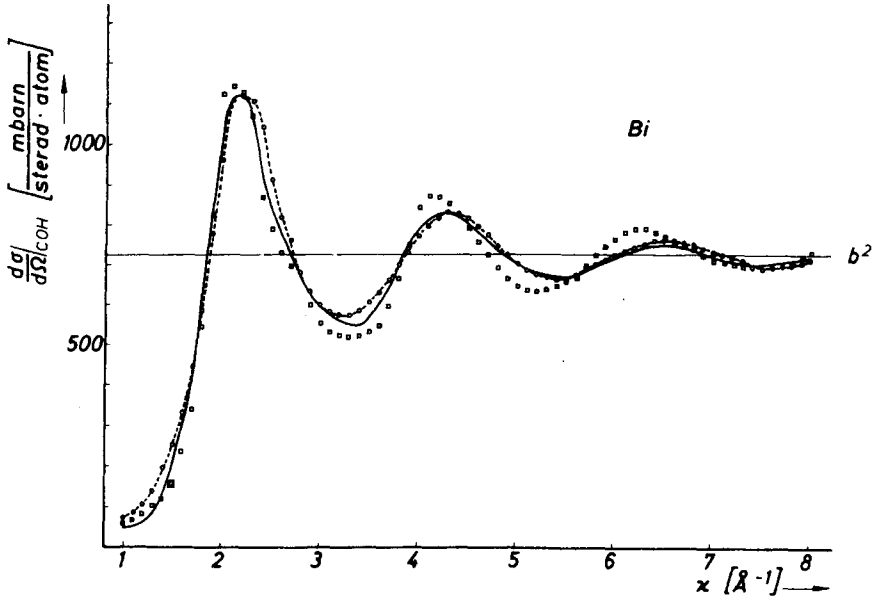

FIGURE 1a Molten Bi: Coherent scattering cross section.
—— T = 800°C; □ T = 300°C according to Ref.[24];
--o--o Hard Sphere Model.

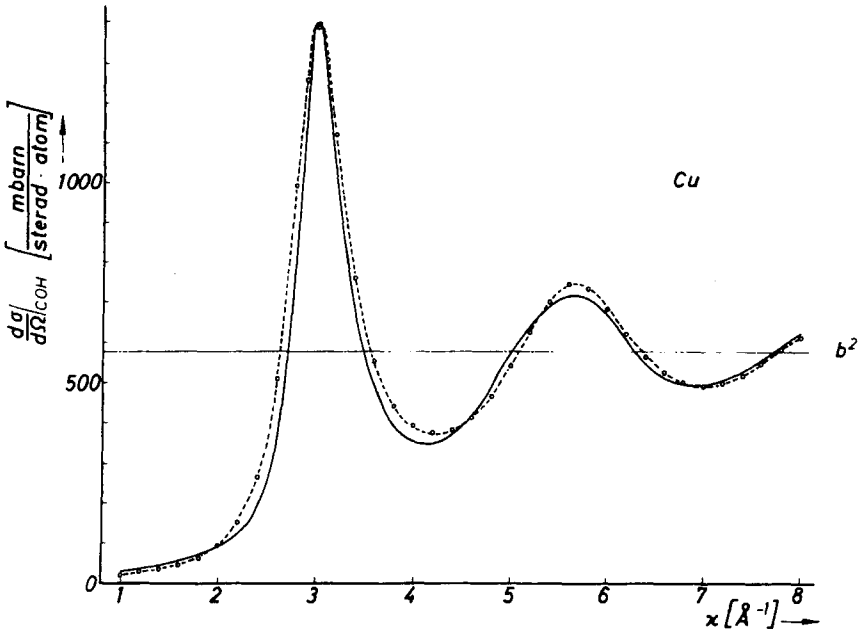

FIGURE 1b Molten Cu: Coherent scattering cross section.
T = 1100° C;
--o--o H.-S. Model.

the results of X-ray diffraction measurements from Isherwood[23] at 670° C. In contrast to the measurements at 300° C, the maxima and minima are not so strong because of the thermal motion of atoms. The additional maximum at $\kappa = 2.82$ Å^{-1}, which was observed in Ref.[23] just above the melting point has nearly fully vanished at a temperature of 800° C. This significant property of the intensity pattern is always observed in the intensity curve of liquid antimony. According to Ref.[25], this effect is explained by the fact that covalent bonds occur in these liquids in addition to the metallic bond.

The coherent scattering cross section of liquid Cu is in agreement with the results in[18]. The intensity pattern has its first maximum at $\kappa = 3.0$ Å^{-1}, its height $\left.\frac{d\sigma}{d\Omega}\right|_M = 1.39$ barn/atom is in agreement with data from Waseda[26].

In Figs. 1a and 1b the experimental values for $\left.\frac{d\sigma(\kappa)}{d\Omega}\right|_{COH}$ are compared with those of a hard-sphere model, calculated according to Ashcroft and Lekner[27] and plotted in these figures with dashed lines.

For liquid Bi at 800° C the best fit could be obtained with a diameter of 2.95 Å for the hard spheres and a packing density of 34%. These values are in agreement with data from Isherwood[23]. Differences between experiment and hard-sphere model appear in the range of the additional maximum mentioned above. This part of the intensity pattern cannot be described with the model of randomly distributed hard spheres.

The best fit for molten Cu was obtained with a diameter of 2.25 Å and a packing density of 46%. As shown in Fig. 1b, the differences between the experimental and calculated curves increase with increasing κ-values. The oscillations of the calculated curve are less damped and more displaced the greater the κ-values are. These differences in κ-space are caused by the fact that in real space at certain atomic distances the hard-sphere potential deviates appreciably from the real potential of the atoms in the melt.

2 Alloys of the Bi-Cu system

In Figs. 2a to 2i the experimental values of the coherent scattering cross section, normalized by Eq. (11), are plotted for several alloys in the momentum range 1 Å^{-1} < κ < 8 Å^{-1} on an absolute scale. The values of $\langle b^2 \rangle$ are represented by horizontal lines.

The position of the first intensity maximum of the alloys with 90 and 80 at.% Bi and with 90 and 80 at.% Cu, respectively, is the same as with the corresponding pure elements, but the height of the first maximum decreases with increasing concentration of the second component. The coherent scattering cross sections of the alloys with 30, 40, 50, and 60 at.% Cu show first intensity maxima, each of which consists of two partial maxima. A similar splitting of the first maximum of the intensity pattern was also

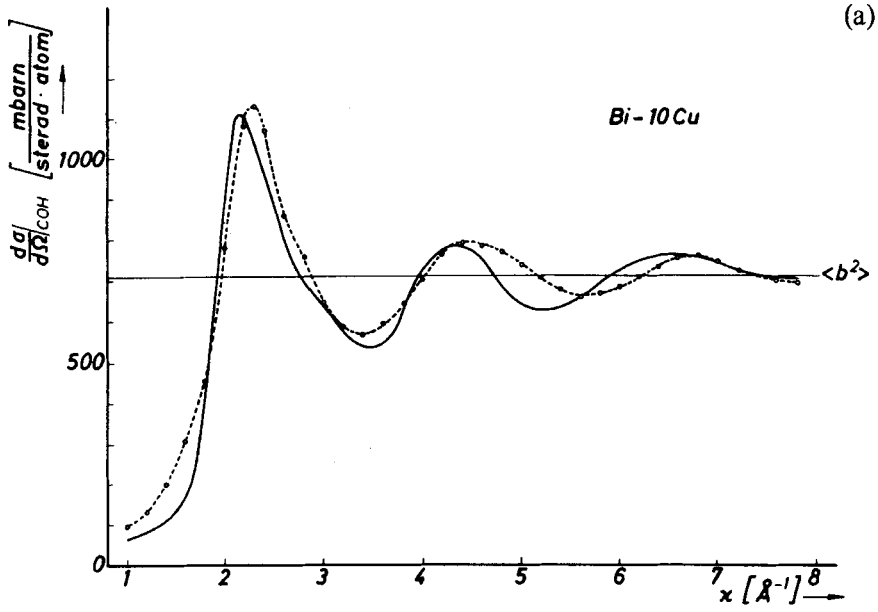

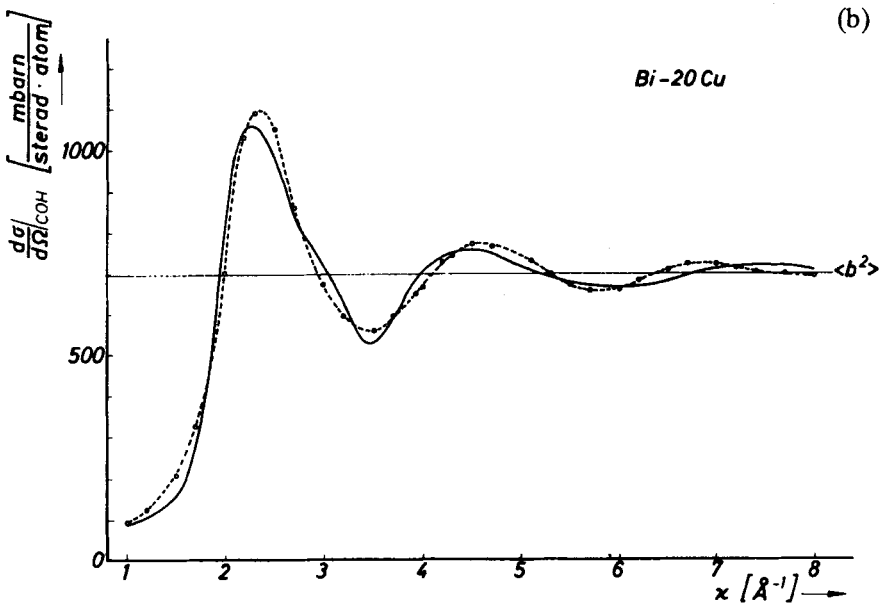

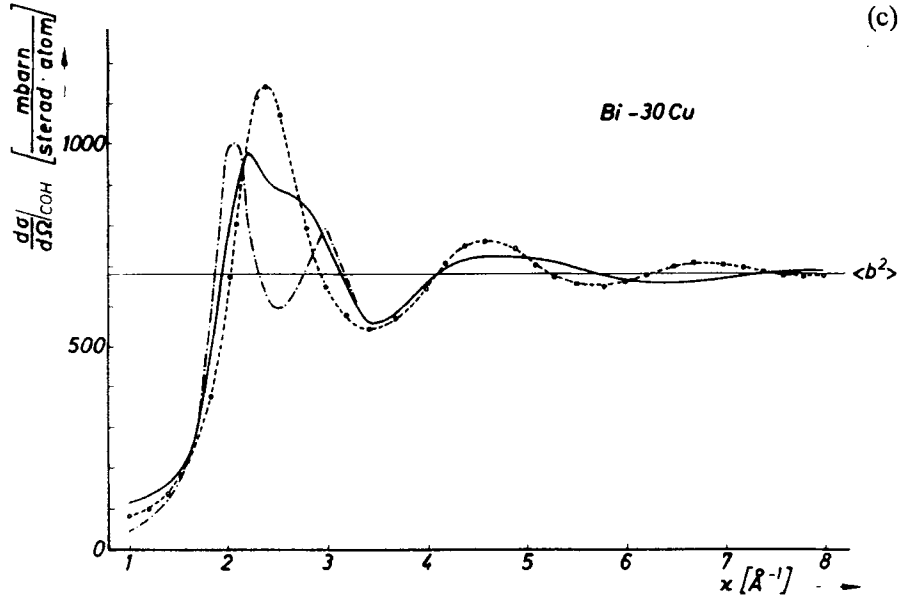

FIGURE 2a–2c Bi-Cu system: Coherent scattering cross section.
— experimental; --o-- H.-S. Model;
–·–·– Total segregation.

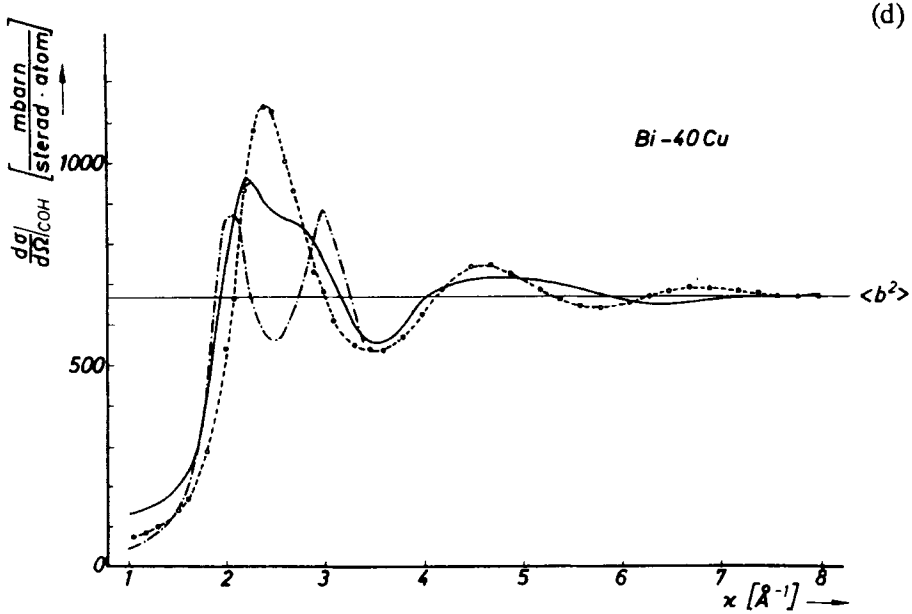

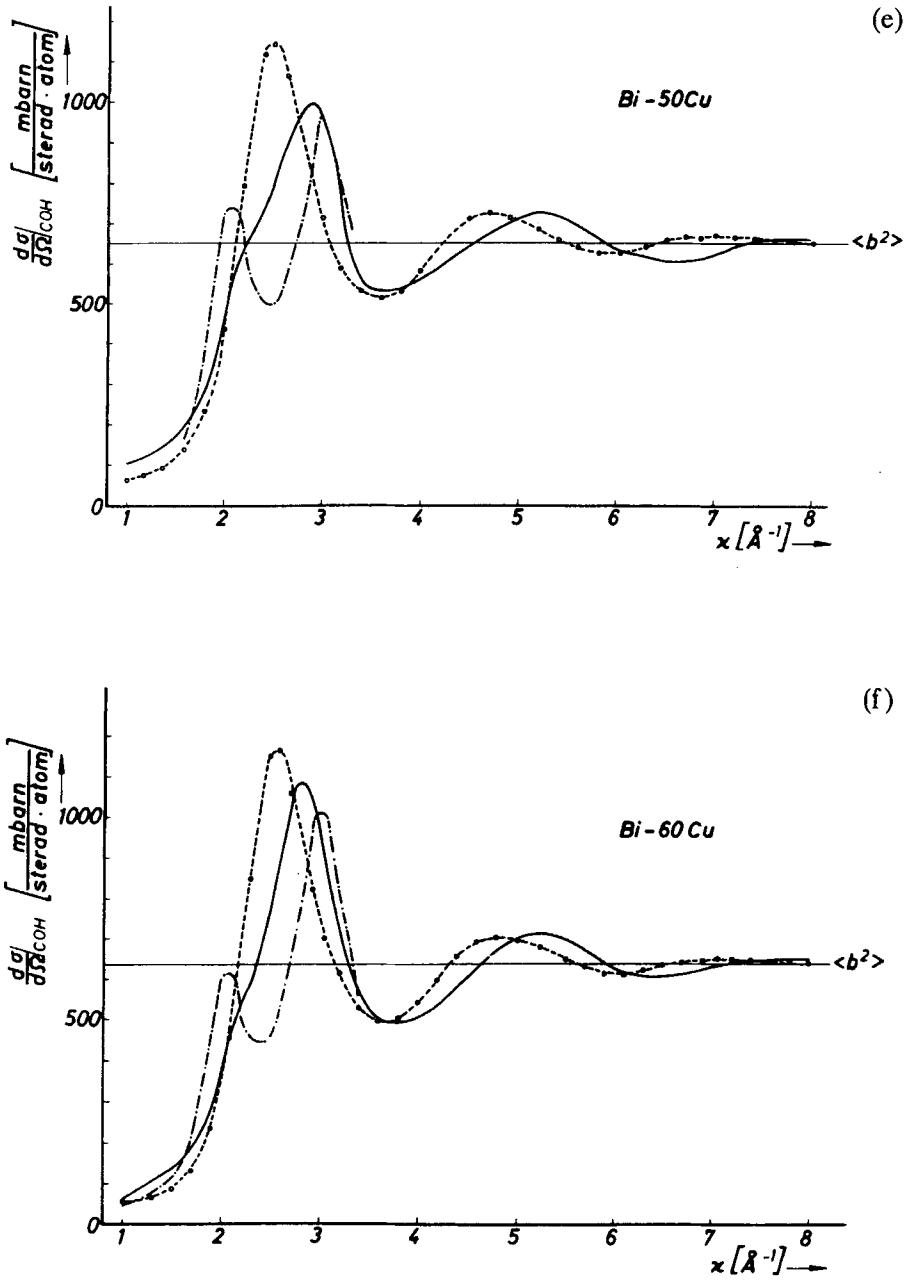

FIGURE 2d–2f Bi-Cu system: Coherent scattering cross section.
— experimental; --o-- H.-S. Model;
–·–·– Total segregation.

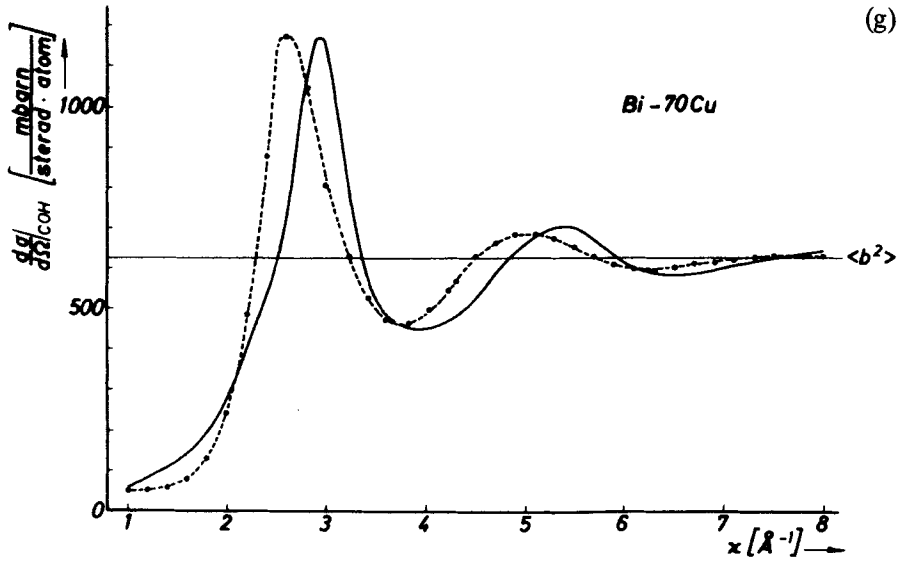

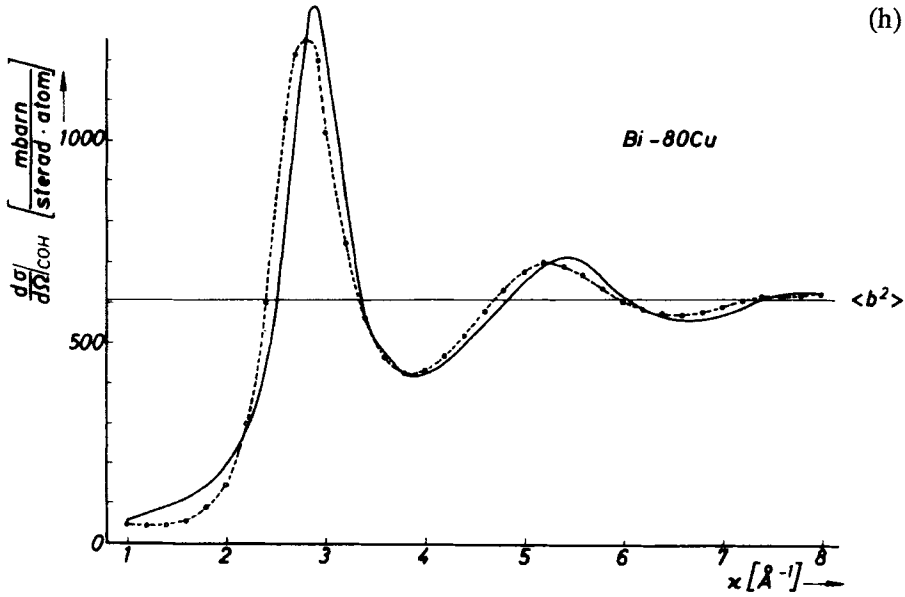

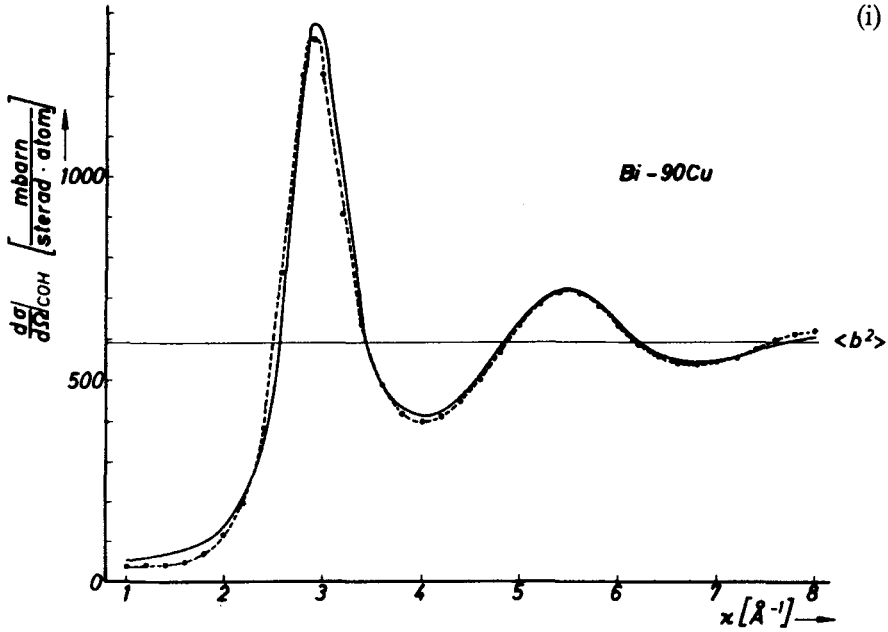

FIGURE 2g–2i Bi-Cu system: Coherent scattering cross section.
— experimental;
--o-- H.-S, Model.

observed in Ref.[18] in the Cu-Sb system in the concentration range between 52 and 80 at.% Sb.

2a Comparison of the experimental intensity curves with two models

In the following sections α and β the experimental coherent scattering cross sections will be compared with the model of complete segregation, on the one hand, and with a hard-sphere model for binary liquid mixtures, on the other.

α Model of total segregation

As pointed out in Ref.[28], the splitting of the first intensity maximum is typical for binary melts showing a tendency to segregation. To estimate the degree of segregation, a coherent scattering cross section is defined for total segregation; this can be calculated from the cross sections of the pure elements as follows:

$$\left.\frac{d\sigma(\kappa)}{d\Omega}\right|_{COH}^{T} = c_{Bi}\left.\frac{d\sigma(\kappa)}{d\Omega}\right|_{COH}^{Bi} + c_{Cu}\left.\frac{d\sigma(\kappa)}{d\Omega}\right|_{COH}^{Cu} \qquad (13)$$

The intensity curves for complete segregation $\left.\frac{d\sigma(\kappa)}{d\Omega}\right|_{COH}^{T}$ were calculated for the alloys between 30 and 60 at.% Cu, and they are plotted in Figs. 2c–f with dash-dotted lines. The clear splitting of the first maximum of the intensity curves into two interference maxima corresponding to Cu-Cu or Bi-Bi atomic distances is due to the difference of the atomic radii of Cu and Bi ($r_{Cu} = 1.28$ Å, $r_{Bi} = 1.82$ Å). The splitting of the first maximum into two partial maxima becomes very distinct for the concentrations where the Cu and the Bi atoms contribute almost equally to the intensity. The two partial maxima show the same height for the alloy containing 40 at.% Cu. For the alloy containing 50 at.% Cu the partial maximum corresponding to the Cu-Cu distance already dominates, even though the scattering length of Bi is greater than the scattering length of Cu (Figs. 2d and 2e).

The experimental values, compared with those calculated for complete segregation, show that the splitting of the first intensity maximum in two partial maxima is only weak. This fact can be explained by the existence of "mixed" distances between Cu and Bi atoms, which, of course, are always present within the melt if there is no total segregation. The intensity maxima corresponding to these "mixed distances" are placed between the intensity maxima of the pure elements. The smearing of the splitting of the first intensity maximum can be explained in that complete segregation is reduced in favour of short-range segregation at the atomic level. This phenomena will be treated in detail in another paper[10].

β Hard-sphere model

According to Eq. (7), the scattering power of a binary liquid alloy is described completely by the three partial structure factors $a_{11}(\kappa)$, $a_{22}(\kappa)$, $a_{12}(\kappa)$, which can be calculated in the hard-sphere approximation following Ashcroft and Langreth[30]. The corresponding parameters are obtained from the pure elements. Using Eq. (6) and (7) the coherent scattering cross section was determined and plotted in Figs. 2a-i.

It follows that the measured intensity of the alloys containing 90 and 80 at.% Cu can be described by a random mixture of hard spheres. The coherent cross section of the alloys containing 10 and 20 at.% Cu are in agreement with the results of the hard-sphere model; in the momentum range of the first intensity maximum there is rather good agreement but in the range $\kappa > 4$ Å^{-1} deviations between experiment and hard-sphere model are found. In the concentration range between 30 and 70 at.% Cu the coherent scattering cross section cannot be described by the hard-sphere model (Figs. 2c-g): in the range of the main maximum, the intensity patterns always lie between the extreme conceptions of complete segregation and statistical distribution.

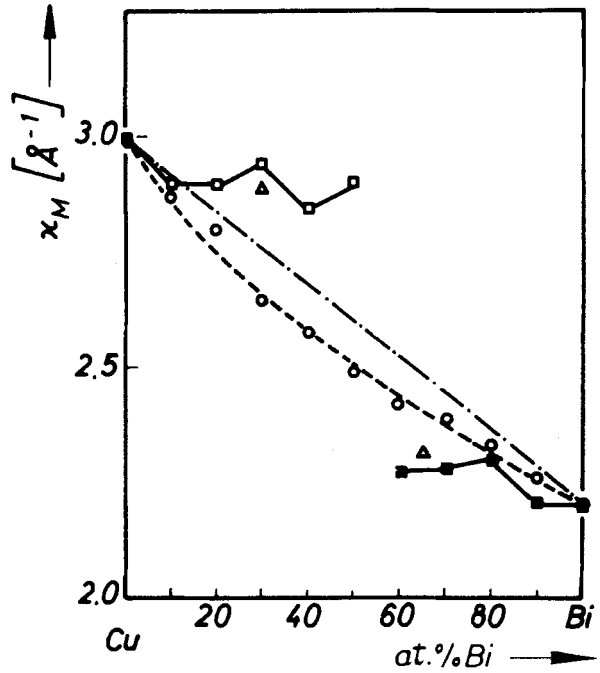

FIGURE 3 Bi-Cu system: Position of main maximum.
□ present work; partial maximum at κ = 3.0 Å^{-1}
■ present work; partial maximum at κ = 2.2 Å^{-1}
△ exp. according to Ref.[8].
o calculated according to H.-S. Model.

2b. Main maximum of the intensity curves

In Fig. 3 the position κ_M of the main intensity maximum is plotted versus the Bi concentration. The positions of the partial maxima (□, ■) are nearly independent of concentration. Values of κ_M(△) for alloys containing 70 and 35 at.% Cu were given already in[8] and are in agreement with those of the present work. In Fig. 3 the values of $\kappa_M(0)$ according to the hard-sphere model are plotted with a dashed line. The shape of this curve differs from the statistical line which would appear if the two species of atoms had the same scattering power.

2c. Radius r_1 of the first coordination sphere

The values of the radius r_1 of the first coordination sphere were taken from the total pair correlation function g(r) and are plotted in Fig. 4 versus the Bi concentration. The values of the pure elements are r_1^{Cu} = 2.55 Å and r_1^{Bi} = 3.27 Å, in agreement with values given in Refs.[18,25]. To calculate the radius r_1 for several models, the atomic distances which occur in the alloy have to be weighted according to the concentration and scattering power of the cor-

responding species of atoms[31]. In the case of complete segregation, the radius r_T is defined as follows:

$$r_T = \frac{c_1 b_1^2 N_1^1 r_1^1 + c_2 b_2^2 N_1^2 r_1^2}{c_1 b_1^2 N_1^1 + c_2 b_2^2 N_1^2} \tag{14}$$

with r_1^1, r_1^2 and N_1^1, N_1^2 = radius r_1 and coordination number N_1 of the pure element 1,2.

In the case of random distribution of the atoms, the radius r_S is calculated from Eq. (15) using for the mixed distance $r_1^{1,2}$ the relation $r_1^{1,2} = (r_1^1 + r_1^2)/2$:

$$r_s = \frac{c_1 b_1 r_1^1 + c_2 b_2 r_1^2}{\langle b \rangle} \tag{15}$$

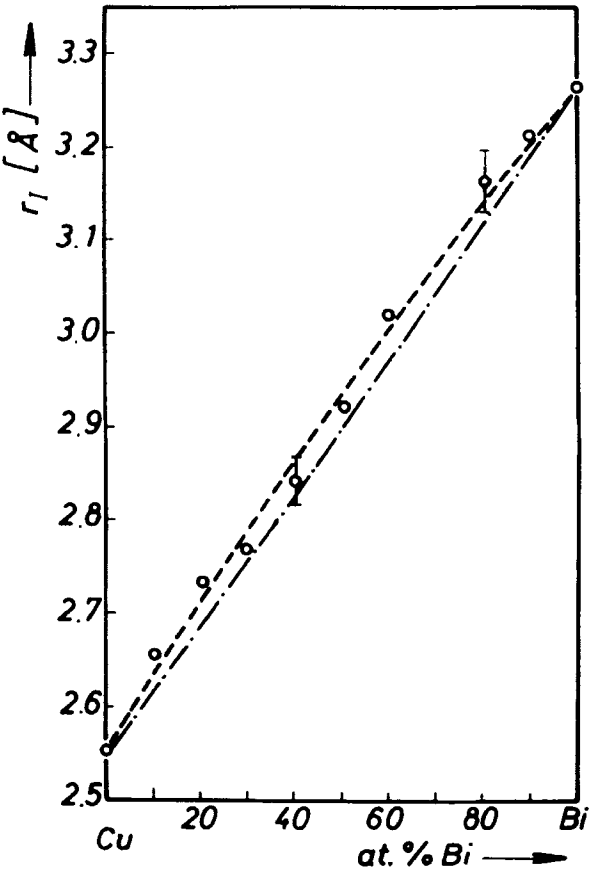

FIGURE 4 Bi-Cu system: Radius r_1 of the first coordination sphere.
---- Statistical distribution (r_S)
–·–· Total segregation (r_T)
o exp.

From Eqs. (14) and (15) it follows that the difference Δr is:

$$\Delta r = r_T - r_S = \frac{c_1 c_2 b_1 b_2 (b_1 N_1^1 - b_2 N_1^2)(r_1^1 - r_1^2)}{\langle b \rangle \cdot (c_1 b_1^2 N_1^1 + c_2 b_2^2 N_1^2)} \tag{16}$$

It is clear that the values of Δr can be greater or less than zero depending on the values of $b_i N_I^i$ and r_I^i. Thus in systems with a tendency to segregation, the experimental values r_I can lie above or below of the curve calculated according to Eq. (15) for the statistical distribution.

For the Bi-Cu system it follows that $b_{Bi} N^{Bi} < b_{Cu} N^{Cu}$, $r_I^{Bi} > r_I^{Cu}$. The experimental values of r_I thus should be below the curve calculated for r_S if these melts show a tendency to segregation. In Fig. 4 the radii r_T and r_S are also plotted versus the Bi concentration. From Eq. (16) the maximum calculated value of Δr is 0.03 Å with the experimental error for the determination of r_I being 0.05 Å. The observed values for r_I lie above as well as below the curve for the statistical distribution of the atoms of both kinds. Regarding the experimental error, it cannot be deduced from Fig. 4 that liquid Bi-Cu alloys are melts with a tendency to segregation. Finally, it should be mentioned that in the Al-In[32] and Al-Sn[33] systems the experimental values of r_I lie above the statistical curve.

2d. Number of atoms N_I in the first coordination sphere

The calculation of the area below the first maximum of the atomic distribution function was performed by using the tangent method[34]. The values of N_I thus obtained are plotted in Fig. 5 versus the Bi concentration. The coordination numbers of the pure elements are $N_I^{Cu} = 9.8$ and $N_I^{Bi} = 7.5$ at 800°C, in good agreement with values of Refs.[18,23]. The dashed line in Fig. 5 represents the curve expected for the case when the atoms occur in the first coordination sphere in a statistical distribution appropriate to their concentration ratio. As shown in Fig. 5, the alloys with 90 and 80 at.% Bi and Cu respectively exhibit random distribution of atoms within experimental error. The alloys in the concentration range between 30 and 70 at.% Bi however, show a considerable positive deviation from the statistical line. According to Ref.[1], it follows that the melts of the Bi-Cu system show a tendency to segregation in this concentration range. The tendency to segregation derived in the present work for molten Bi-Cu alloys will be investigated in more detail in Ref.[10], where the size, composition and concentration of the segregated regions will be determined. At this point Ref.[18] should be mentioned once more, where calculations were performed for the electrical resistivity of molten Bi-Cu alloys over the entire concentration range on the basis of a statistical distribution of the Bi and Cu atoms. The assumption of the hard-sphere model in the concentration range between 30 and 70 at.% Cu is not justified on the basis of the results of the present work.

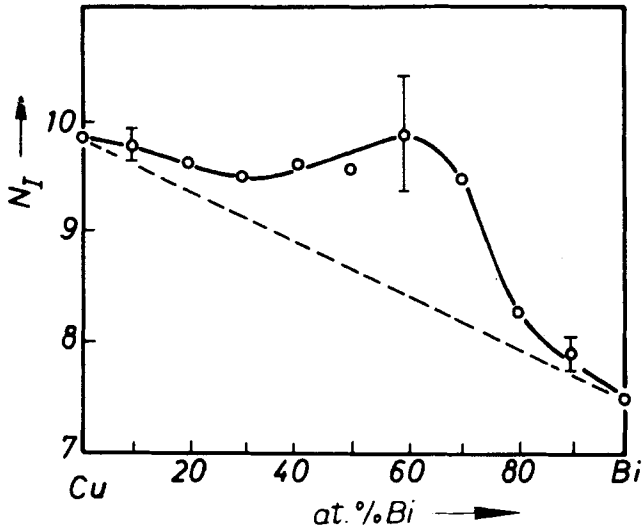

FIGURE 5 Bi-Cu system: Coordination number N_I.

Acknowledgements

We wish to thank the Deutsche Forschungsgemeinschaft, the Kernforschungszentrum Karlsruhe, and the Computer Center of the University of Stuttgart for their support and assistance.

References

1. S. Steeb, *Habilitationsschrift*, Universität Stuttgart, 1969.
2. S. Steeb and H. Entress, *Z. Metallkunde* **57**, 803 (1966).
3. H. Ruppersberg, *Phys. Letters* **46A**, 75 (1973).
4. R. Hezel and S. Steeb, *Z. Naturforschg.* **25a**, 1085 (1970).
5. J. Höhler, Dissertation, Universität Stuttgart, 1975.
6. H. Brumberger et al., *Phys. Rev. Lett.* **19**, 555 (1967).
7. G. Bauer and F. Sauerwald, *Wiss. Z. Univ. Halle*, Math.-N. X/5, 1029 (1961).
8. S. Takeuchi, K. Suzuki *et al.*, in "Properties of Liquid Metals", S.69, ed. S. Takeuchi (Taylor u. Francis, London 1973).
9. H. Ebert, J. Höhler, and S. Steeb, *Z. Naturforschg.* **29a**, 1890 (1974).
10. W. Zaiss, S. Steeb and G. Bauer, *J. Phys. Chem. Liquids* **5**, 89 (1976).
11. W. Marshall and S. W. Lovesey, "Theory of Thermal Neutron Scattering" (Oxford 1971).
12. P. A. Egelstaff, in "Properties of Liquid Metals" S.147, ed. P. D. Adams, H. A. Davis and S. G. Epstein (Taylor u. Francis, London 1967).
13. T. E. Faber and J. M. Ziman, *Phil. Mag.* **11**, 153 (1965).
14. W. Zaiss, Dissertation, Universität Stuttgart, 1975.
15. Table of Coherent Neutron Scattering Amplitudes (comp. Febr. 1972, M.I.T. Shull C. G.).
16. J. P. Niklaus, R. Simson, W. Triftshäuser, and W. Schmatz, *Z. Phys.* **190**, 295 (1966).
17. G. E. Bacon, "Neutron Diffraction" (Clarendon Press Oxford 1962).
18. W. Knoll and S. Steeb, *Phys. and Chem. Liquids* **4**, 39 (1973).
19. K. D. Rouse and M. J. Cooper, *Acta Cryst.* **A26**, 682 (1970).
20. I. A. Blech and B. L. Averbach, *Phys. Rev.* **137A**, 1113 (1965).

21. G. Placzek, *Phys. Rev.* **86A**, 377 (1952).
22. J. Krogh-Moe, *Acta Cryst.* **9**, 951 (1956).
23. S. P. Isherwood and B. R. Orton, *Phil. Mag.* **17**, 561 (1968).
24. M. Weber, Diplomarbeit, Universität Stuttgart, 1974.
25. H. P. Lamparter, S. Steeb, and W. Knoll, *Z. Nat. forschung* **31a**, 90 (1976).
26. Y. Waseda and K. Suzuki, in "Properties of Liquid Metals" S.37, see Ref.[8].
27. N. W. Ashcroft and J. Lekner, *Phys. Rev.* **145**, 83 (1966).
28. R. Hezel, Dissertation, Universität Stuttgart, 1968.
29. M. H. Hansen and K. Anderko, Constitution of Binary Alloys, McGraw Hill Book Co., New York (1958).
30. N. W. Ashcroft and D. C. Langreth, *Phys. Rev.* **156**, 685 (1967).
31. R. Hezel and S. Steeb, *Phys. Kondens. Mat.* **14**, 307 (1972).
32. J. Höhler and S. Steeb, Z.Nat.forschg. **30a**, 771 (1975).
33. R. Hezel and S. Steeb, *Phys. kond. Materie* **14**, 314 (1972).
34. C. J. Pings, in "Physics of Simple Liquids", S.388 see Ref.[12].